NAU Journal of Civil Engineering (NAUJCVE) March/April 2025
Nnamdi Azikiwe University Journal of Civil Engineering (NAUJCVE)

Volume-3, Issue-2, pp-94-104
www.naujcve.com
Research Paper Open Access

Investigation on the Compressive Strength property of Rubberized GGBFS Geopolymer Concrete

Orie O. U[1] and Akingbade Adebayo S[2]

[1,2]*Department of Civil Engineering, University of Benin, Benin City, Nigeria*

***Corresponding Author**: debayo2k1@gmail.com*

ABSTRACT : *This study examines the compressive strength development of rubberized ground granulated blast furnace slag (GGBFS) geopolymer concrete (GPC). Varying proportions of rubber crumbs were used as partial aggregate replacements, with alkaline activators comprising sodium silicate (silica-to-sodium oxide ratio of 3:1) and 4M sodium hydroxide to aid geopolymerization. A two-part geopolymer method was adopted, and mix design was guided by prior studies due to the absence of standardized GPC codes. Chemical analyses of slag and rubber crumbs were conducted. Following BS 1881: Part 118, cube samples of 100mm³ were molded and then oven-cured (25°C–60°C) for 7, 14, and 28 days. Compressive strength tests showed a decline in strength with increased rubber content, though optimized mixes maintained structural integrity. At 7 and 28 days, 3% rubber mixes recorded the highest strengths (0.157 MPa and 0.156 MPa respectively). However, unrubberized GPC displayed lower strength than OPC (~20 MPa), attributed to aluminosilicate limitations. FTIR analysis revealed weakly bonded phases like Clinochlore and Marialite, indicating a lack of essential Si^{4-} and Al^{3+} ions. The findings demonstrate the potential of recycled steel slag and rubber in sustainable construction, despite strength-related challenges*

KEYWORDS: *Geopolymer, Slag, Tyre, Compressive strength, Construction*

Date of Submission: 09-04-2025 Date of acceptance: 16-04-2025

I. INTRODUCTION

Concrete, the second most consumed material after water, plays a vital role in modern infrastructure but relies heavily on cement. Due to environmental concerns, researchers are actively exploring alternative materials to enhance its sustainability and performance. A study by John and Smith [1] highlights the integration of industrial by-products in concrete to reduce its carbon footprint while enhancing mechanical properties. Studies indicate that global cement production reached approximately 2.8 billion metric tons in 2020 [2]. Despite its widespread use, the cement industry poses major environmental challenges, with Portland Limestone Cement (PLC) production consuming high energy and emitting pollutants - contributing about 5% of global CO_2 emissions. Other associated concerns include biodiversity loss, reduced crop productivity, ozone depletion, and ocean acidification [3] [4] [5]. As such, sustainable alternatives to PLC have become a critical focus of research. One promising avenue is the use of supplementary cementitious materials (SCMs) such as ground granulated blast furnace slag (GGBFS), silica fume, natural zeolite, metakaolin, and fly ash (FA) [6] which has so evolved into geopolymer concrete (GPC) essentially with potential to address environmental concerns. GPC primarily consists of two components: a source material and an alkaline activator. The choice of source material depends on factors such as cost, availability, and intended application [7]. High-performance, low-impact GPC can be produced using by-product materials combined with waste products such as quarry dust, agricultural waste, or recycled aggregates.

Geopolymer concrete offers a sustainable alternative. Sodium hydroxide, sodium silicates, and similar sodium-based high alkaline reagents are the most used activators in GPC [8]. One of the source materials rich in aluminosilicates used in GPC is the GGBFS - a by-product of the steel manufacturing industry. Approximately 300 million metric tons of GGBFS are produced annually, with projected

www.naujcve.com. All Rights Reserved 2025.

growth of 1.6% by 2025, contributing to unsustainable waste management challenges [9]. In a study by Nath and Sarker [10], it was shown that GGBFS-FA based GPC cured at ambient temperature achieved relatively more ductility comparable to those of normal PLC concrete. In another literature, the effect of use of combination of source materials of FA, GGBFS, Silica Fume and Metakaolin (MK) was studied, and it was found that highest compressive strength and flexural strength was achieved with higher per centage of GGBFS and MK respectively [11]. Glasby, et al., [12] presented findings on geopolymer concrete's application in aircraft pavements, noting a 40% reduction in carbon emissions compared to traditional methods and exceptional durability under heavy loads. Similarly, Mohabbi and Dener [13] examined the compressive strength and microstructure of alkali-activated slag-based cements exposed to elevated temperatures. Results demonstrated a 75% retention of compressive strength after exposure to 800°C, confirming its high thermal resistance.

While prior researches have demonstrated the efficacy of GGBFS-based GPC in enhancing workability and strength, the incorporation of locally available waste materials, such as recycled tires, remains underexplored. The potential of using waste materials, including tire dust, to improve its mechanical and durability properties is critical. Reddy, *et al.*, [14] investigated the durability of fly ash–based geopolymer concrete in marine environments. Their findings highlighted that the concrete exhibited over 80% strength retention after prolonged exposure to chloride-rich conditions, demonstrating significant resistance to chemical attack. Ahmed *et al.*, [15] demonstrated that incorporating rubber particles in geopolymer composites enhances ductility and crack resistance, offering a promising avenue for sustainable construction practices. Current studies highlight the potential of waste tires, whether as crumbs, dust, or fibers, in concrete production [16]. However, there is a notable knowledge gap in understanding the mechanical performance of GGBFS-based GPC incorporating tire dust as a pozzolan. Thus, this present research seeks to address this gap by developing GPC incorporating GGBFS as the base material, with partial replacement using tire dust as a pozzolan. The mechanical properties of rubberized GGBFS GPC were experimentally investigated with a focus on compressive strength.

II. MATERIALS AND METHODS

2.1 Materials

Coarse aggregates: Coarse aggregates significantly influence the mechanical properties of concrete, comprising 40% to 50% of its total volume. Proper grading and particle shape enhance bonding strength and durability. Aggregate type and quality are important in achieving optimal mechanical performance. Well-graded aggregates with angular shapes improved interlocking and reduced void spaces thereby enhancing compressive. In this study, coarse aggregates were sourced from a quarry site and sieved through a series of British standard sizes (19mm to 0.075mm).

Fine Aggregates: Fine aggregates play a critical role in the workability and strength of concrete, constituting approximately 30% to 40% of its total volume. Proper gradation and particle size distribution contribute to uniformity, improved compaction, and reduced voids in the concrete mix. Fine aggregates, primarily composed of river sand, were graded according to IS 383 (1970). Particle sizes ranged from 4.75mm to 75µm.

Ground Granulated Blast Furnace Slag: Ground granulated blast furnace slag is a glassy, granular material formed as a by-product of iron and steel production. The physical characteristics of GGBFS vary based on its chemical composition and production methods, ranging from coarse, popcorn-like structures larger than 4.75mm (No. 4 sieve) to dense, sand-sized particles. The material's specific gravity is approximately 2.90, while its average particle size, depending on the source, is typically between 1mm and 1.5mm. For this study, GGBFS was sourced from Inner Galaxy Steel Company in Abia State and Ajaokuta Steel Industry in Kogi State. The material was processed by grinding it into a fine powder, to ensure suitability for geopolymer concrete applications. The specific GGBFS used in this study was subjected to qualitative and quantitative chemical analysis to determine its exact composition. Table 2.1 presents the detailed chemical components of the GGBFS used, highlighting key elements such as SiO_2, Al_2O_3, and CaO, which play a crucial role in the geopolymerization process.

Tyre Dust

Tyre dust (crumbs) used in this study was sourced from waste automobile tyres shredded and grounded into fine particles. The percentage composition of tyre forms the basis for understanding the interaction of tyre crumbs within the geopolymer matrix. The tyre crumbs prepared for this study were subjected to quantitative analysis, with the results summarized in Tables 2.1. This analysis highlights the chemical and structural characteristics of the tyre crumbs,

www.naujcve.com. All Rights Reserved 2025.

including key compounds such as carbon black, methylene, and transitional metal carbonyls. The use of tyre crumbs in GPC has been recognized for its potential to enhance deformation properties and sustainability. By recycling waste tyres into construction materials, this study aligns with broader environmental objectives while exploring the effects of tyre dust on the mechanical properties of geopolymer concrete.

Table 2.1 Quantitative Analysis of Rubber Crumbs

Phase Name	Formula	Fig. of Merit	Phase Registration Detail	Space Group	DB Card Number
Hematite	Fe_2O_3	2.946	Import(PDF-4 Minerals 2021)	167: R-3cH	00-001-1053
Bixbyite	$Fe_{2+3}O_3 \cdot Mn_{2+3}O_3$	3.398	Import(PDF-4 Minerals 2021)	206: Ia-3	00-002-0886
Graphite	C	0.792	Import(PDF-4 Minerals 2021)	147: P-3	00-001-0640
Marialite	$(Na_{3.21}Ca_{0.68}K_{0.11})Si...$	1.436	Import(PDF-4 Minerals 2021)	87: I4/m	01-070-6156
Clinochlore	Al-Fe-SiO_2-OH	2.242	Import(PDF-4 Minerals 2021)		00-002-0022
Quartz	SiO_2	1.661	Import(PDF-4 Minerals 2021)	154: P3221	00-001-0649

2.2 Method

Specimen Preparation and Testing

The laboratory works for this research was conducted at the Civil Engineering Laboratory, University of Benin, under ambient temperatures between 22°C and 26°C. The alkaline activator consisted of sodium silicate and sodium hydroxide solutions. The activator was produced using a blend of sodium silicate with caustic soda. Sodium hydroxide (4M concentration) was prepared by dissolving NaOH flakes in distilled water. Sodium silicate (Na_2SiO_3) had a silica-to-sodium oxide weight ratio of 3:1. Distilled water, free from harmful chemicals and microorganisms, was used throughout the experiment.

The preparation of geopolymer concrete (GPC) generally involves two distinct methods: the one-part geopolymer and the two-part geopolymer preparation methods. While the one-part geopolymer method involves use of solid alkaline activators mixed with dry materials, the two-part geopolymer method was used on this work. It involved mixing the liquid alkaline activator solutions (sodium hydroxide and sodium silicate) prepared 24 hours earlier, with the dry binders and the dry aggregates, followed by the slow addition and mixing with appropriate volume of clean water to achieve homogeneity. Due to the lack of standardized design codes for GPC, no systematic guidelines were followed. Consequently, the mix design used in this research, as illustrated in Fig. 2.1, was adapted from similar work. Control samples without rubber crumbs content alongside samples containing varying percentages of rubber crumbs were molded into cubes (100mm x 100mm x 100mm) following BS 1881: Part 118. The variation in rubber crumbs content aimed to identify the optimal properties of GPC. To achieve enhanced strength, curing was conducted at high and regulated temperature between 25°C to 60°C. Compressive strength test was then determined on cube specimens through testing at 7, 14, and 28 days. Specimens were tested to failure on a universal testing machine at a constant load rate.

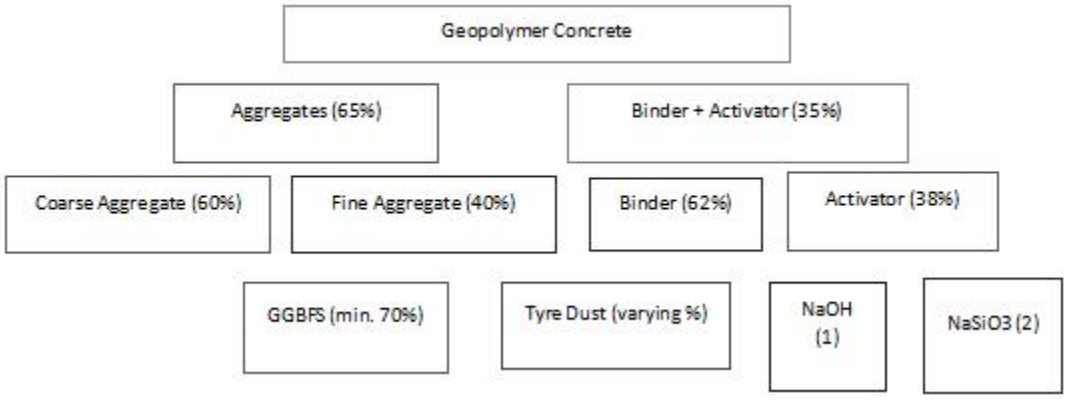

Fig. 2.1 Geopolymer Concrete Mix Design - Adapted from Ediae and Okovido, [17]

III. RESULTS AND DISCUSSION

The results obtained from the experimental investigation focuses on compressive strength of rubberized GPC and microstructural and chemical evaluations with particular attention to the chemical composition of the GGBFS. Essentially, the integration of advanced analytical techniques such as FTIR and XRD analyses enhanced understanding of material performance. Furthermore, the sieve analysis results were obtained for fine aggregate, coarse aggregate, slag, and rubber crumbs.

www.naujcve.com. All Rights Reserved 2025.

3.1 Sieve Analysis

The sieve analysis showed that GGBFS had over 80% passing the 0.212 mm sieve, thereby indicating fine particles ideal for geopolymerization and matrix densification. Similarly, both tyre crumbs and granite had 50.35% retained on the 19 mm sieve, thus confirming their suitability as coarse aggregate replacements for structural support and enhanced deformation behavior. Meanwhile, sharp sand demonstrated a well-graded profile, with 55.39% passing the 0.6 mm sieve, consequently promoting good packing, workability, and strength development in the GPC mix. The sieve analysis for slag and rubber crumbs are shown in Fig.s 3.1 and 3.2, respectively.

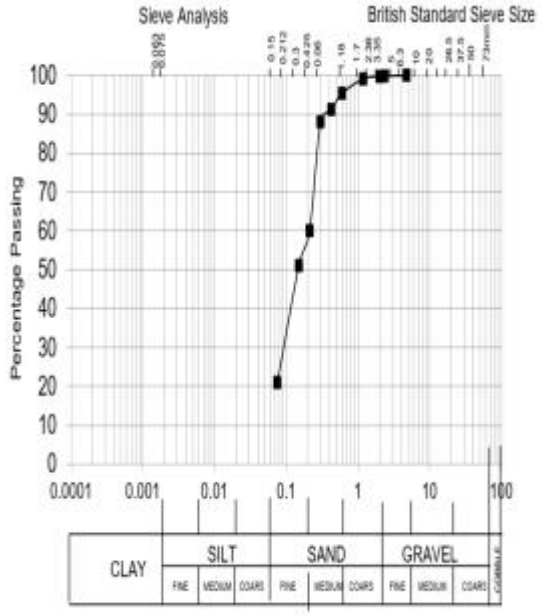

Fig. 3.1:Sieve Analysis Results of GGBFS Powder

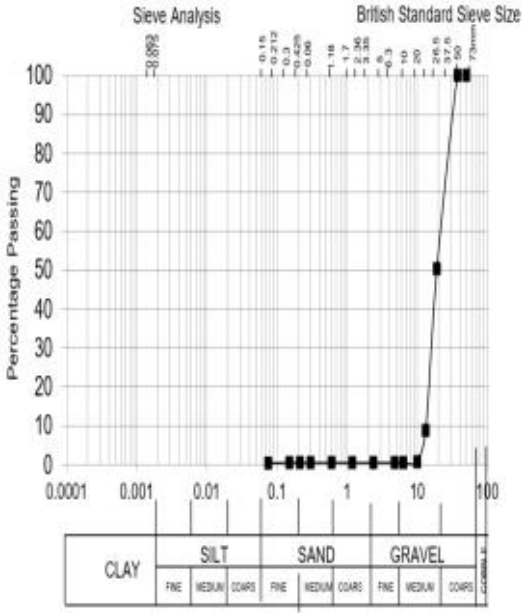

Fig. 3.2: Sieve Analysis Results of Tyre Crumbs

3.2 Chemical Analysis

The chemical composition of GGBFS was analyzed, and the results are presented in Tables 3.1a and 3.1b. The chemical components include SiO_2, Al_2O_3, Fe_2O_3, and trace minerals such as Clinochlore and Marialite. Fig.s 3.3 and 3.4a provide a graphical representation of the qualitative and quantitative analyses respectively, while Fig. 3.4b illustrates the data in a pie chart.

Table 3.1a Qualitative Analysis Results Showing Chemical Components of the GGBFS (Peak List)

No.	2θ, °	d, Å	Height, cps FWHM, °		Int. I, cps°	Int. W, °	Asymmetry	Decay (nL/mL)	Decay (nH/mH)	Size, Å
1	28.84(10)	3.094(10)	750(78)	48.0(2)	38351(186)	51(6)	0.580(4)	0.00(4)	0.00(2)	1.783(8)
No.	2θ, °	Phase Name	Chemical Formula		Card No	Norm. I.	Profile Type	Distribution	Degree of Distribution	
1	28.84(10)	Hematite: 10 4, Bixbyite: 222	Fe_2O_3, $Fe_{2+3}O_3$		00-001-1053	100.00	Split pseudo-Voigt	-	-	
No.	2θ, °	Ring Factor		β Cluster						
1	28.84(10)	-		-						

www.naujcve.com. All Rights Reserved 2025.

Table 3.1b Qualitative Analysis Results Showing Chemical Components of the GGBFS (Components)

Phase Name	Formula	Fig. of Merit	Phase Registration Detail	Space Group	DB Card Number
Hematite	Fe_2O_3	2.946	Import(PDF-4 Minerals 2021)	167: R-3cH	00-001-1053
Bixbyite	$Fe_{2+3}O_3 \cdot Mn_{2+3}O_3$	3.398	Import(PDF-4 Minerals 2021)	206: Ia-3	00-002-0886
Graphite	C	0.792	Import(PDF-4 Minerals 2021)	147: P-3	00-001-0640
Marialite	$(Na_{3.21}Ca_{0.68}K_{0.11})Si...$	1.436	Import(PDF-4 Minerals 2021)	87: I4/m	01-070-6156
Clinochlore	Al-Fe-SiO_2-OH	2.242	Import(PDF-4 Minerals 2021)		00-002-0022
Quartz	SiO_2	1.661	Import(PDF-4 Minerals 2021)	154: P3221	00-001-0649

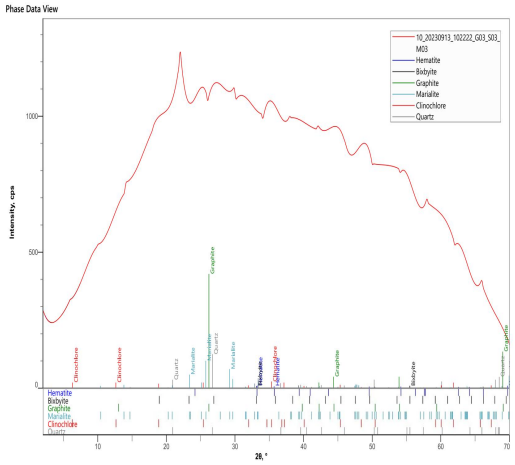

Fig. 3.3: Qualitative Analysis Graph of grinded GGBFS

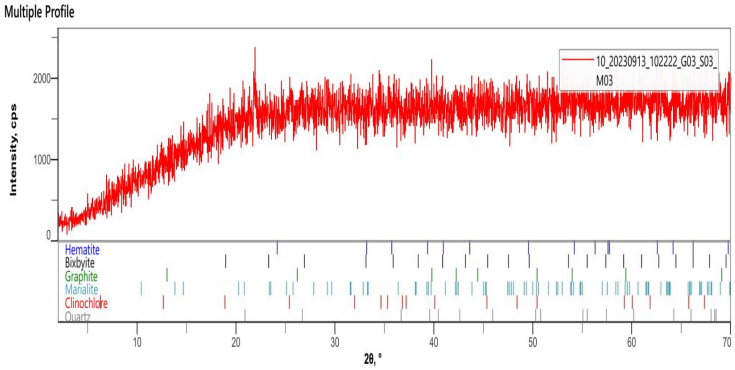

Fig. 3.4a: Quantitative Analysis Result (in Profile Graph) of the GGBFS

Plot of results

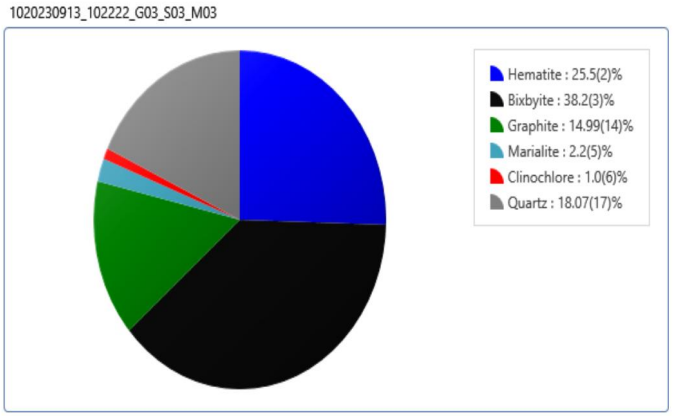

Table of results

Dataset / Weight Fraction,...	Value, Unit	Hematite	Bixbyite	Graphite	Marialite	Clinochlore	Quartz
10_20230913_102222_G03...	0	25.5(2)	38.2(3)	14.99(14)	2.2(5)	1.0(6)	18.07(17)

Fig. 3.4b : Pie Chart Representation of GGBFS Quantitative Analysis

FTIR results for rubber crumbs are shown in Table 3.2 and Fig. 3.5 The analysis identifies functional groups and compounds contributing to the material's properties.

Table 3.2: FTIR Result for Rubber Crumbs

Frequency	Appearance	Bonds	Compounds
3189.13	Weak to medium absorption band	Ammonium ion NH4	Inorganic ion
2914.08	Broad and strong absorption band	C-H stretch	Methylene, Alkenes
2845.85	Sharp and strong absorption band	C-H stretch	Methylene Alkane/Alkyl
2248.97	Medium to strong absorption band	Medial alkyne (disubstituted) C=C	(Alkyne) Acetylene compound
2086.61	Weak to medium absorption band	Transitional metal carbonyls	Carbonyl compounds
1986.00	Weak to medium absorption band	Transitional metal carbonyls	Carbonyl compounds
1536.50	Medium to strong absorption band	Aliphatic nitro compounds	Hetero oxy compound
471.53	Weak to medium absorption band	S-S stretch	Thiols compound. Polysulfide
442.42	Weak to medium absorption band	S-S stretch	Thiol compound. Aryl disulphide

www.naujcve.com. All Rights Reserved 2025.

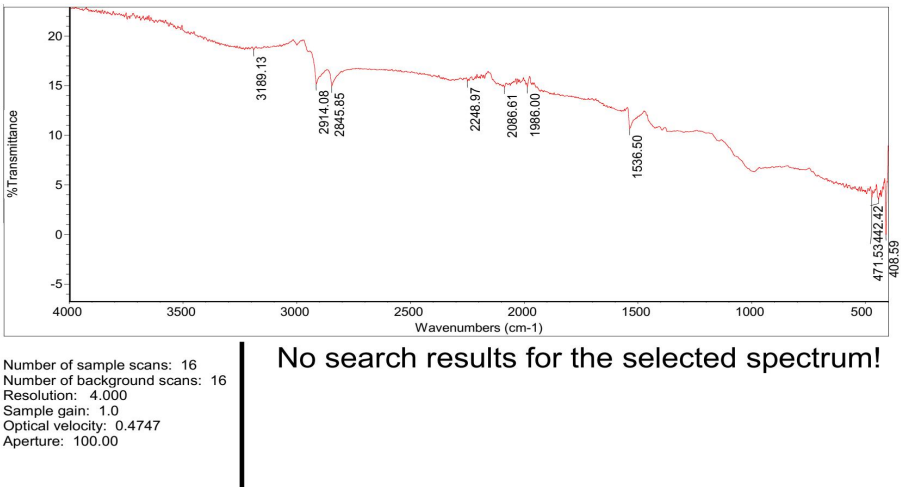

Fig. 3.5 Result of Fourier Transform Infrared Spectroscopy/Radiation of the Rubber Crumbs

3.3 Mechanical Properties

Compressive strength tests were conducted on both unrubberized and rubberized GPC samples. Results are presented in Tables 3.3 and 3.4a. Table 3.4b provides computed averages for each group, with trends indicating systematic reduction in compressive strength as rubber content increased. For instance, at 7 days: 3% rubber samples achieved 0.157 MPa, while 9% rubber samples had 0.109 MPa. Also, at 28 days: 3% rubber samples retained the highest compressive strength (0.156 MPa) among the rubberized mixes.

In comparison with benchmarks, the strength values of unrubberized GPC fall below conventional OPC concrete benchmarks (~20 MPa for similar mix proportions). This deviation highlights the limitations posed by the aluminosilicate composition of the GGBFS used.

The presence of weakly bonded compounds such as Clinochlore and Marialite in the slag contributes to limited geopolymerization. These findings align with FTIR analysis (Table 3.1b), which indicates insufficient Si^{4-} and Al^{3+} ions required for robust cross-linking.

Mini-slump tests revealed that workability decreased with increasing rubber Mini-slump tests revealed that workability decreased with increasing rubber content due to rubber's hydrophobic properties, which reduce the mix's cohesion and flowability. The addition of rubber crumbs disrupts the particle-packing efficiency within the matrix, leading to a higher water demand for similar levels of consistency. This effect is further compounded by the irregular shape and surface texture of rubber particles, which hinder smooth flow during placement. Additionally, as the rubber content increases, the mix exhibits greater segregation tendencies, making it more challenging to achieve uniform distribution of materials. These observations are consistent with findings by Gayathri and Raja [18], who noted a similar reduction in workability in rubberized concrete mixes.

Table 3.3 Compressive Test Result: 100mm x 100mm x 100mm Cube Samples of Unrubberized GPC

7-Day Cured Unrubberized Samples			14-Day Cured Unrubberized Samples			28-Day Cured Unrubberized Samples		
Sample	**Mass (kg)**	**Failure Load (KN)**	**Sample**	**Mass (kg)**	**Failure Load (KN)**	**Sample**	**Mass (kg)**	**Failure Load (KN)**
UR1-7	2.514	2.141	UR1-14	2.541	2.106	UR1-28	2.514	2.363
UR2-7	2.533	1.969	UR2-14	2.561	2.301	UR2-28	2.567	2.286
UR3-7	2.545	1.978	UR3-14	2.551	2.236	UR3-28	2.574	2.249

Where:
URC1-7, URC2-7, and URC3-7 represent unrubberized samples cured for 7 days, while URC1-14, URC2-14, and URC3-14 correspond to those cured for 14 days; similarly, URC1-28, URC2-28, and URC3-28 denote unrubberized samples cured for 28 days.

www.naujcve.com. All Rights Reserved 2025.

Table 3.4a Compressive Test Result: 100mm x 100mm x 100mm Cube Samples of Rubberized GPC

7-Day Cured Rubberized Samples			14-Day Cured Rubberized Samples			28-Day Cured Rubberized Samples		
Sample	**Mass (kg)**	**Failure Load (KN)**	**Sample**	**Mass (kg)**	**Failure Load (KN)**	**Sample**	**Mass (kg)**	**Failure Load (KN)**
RC1-3-7	2.284	1.479	RC1-3-14	2.261	1.514	RC1-3-28	2.214	1.592
RC2-3-7	2.285	1.721	RC2-3-14	2.277	1.621	RC2-3-28	2.220	1.499
RC3-3-7	2.295	1.511	RC3-3-14	2.243	1.711	RC3-3-28	2.236	1.579
RC1-6-7	1.186	1.259	RC1-6-14	1.173	1.110	RC1-6-28	1.142	1.012
RC2-6-7	1.701	1.001	RC2-6-14	1.520	1.231	RC2-6-28	1.116	1.099
RC3-6-7	1.803	1.412	RC3-6-14	1.614	1.143	RC3-6-28	1.147	1.061
RC1-9-7	1.612	1.102	RC1-9-14	1.712	1.012	RC1-9-28	1.621	1.021
RC2-9-7	1.663	1.060	RC2-9-14	1.614	1.061	RC2-9-28	1.556	1.041
RC3-9-7	1.432	1.120	RC3-9-14	1.743	1.011	RC3-9-28	1.513	1.012

Where:

Each RC code represents a specific rubberised sample, following the format: RC[SampleNumber]-[Rubber%]-[CuringDays]. For every curing age (7, 14, and 28 days), three samples were tested at each rubber crumb content level (3%, 6%, and 9%). This naming system helps clearly identify and track the performance of each mix across different curing periods and rubber content levels.

For example,
RC1-3-7 represent sample 1 containing 3% rubber crumbs at Day-7 cured
RC3-9-14 represent sample 3 containing 9% rubber crumbs at Day-14 cured
RC3-9-28 represent sample 3 containing 9% rubber crumbs at Day-28 cured

Table 3.4b Averaged Compressive Test Result Computed from Table 3.4a

Percentage of Tyre Dust in Averaged GPC Samples (%)	Averaged Samples Id	Compressive strength (MPa)	Cured Period (Days)
3	S3-7	0.157	7
6	S6-7	0.122	
9	S9-7	0.109	
3	S3-14	0.162	14
6	S6-14	0.116	
9	S9-14	0.103	
3	S3-28	0.156	28
6	S6-28	0.106	
9	S9-28	0.102	

Where:

Each S-code (e.g., S3-7, S6-14) represents the average result of three rubberized GPC samples with a specific rubber content (3%, 6%, or 9%) cured at 7, 14, or 28 days. For instance, S3-7 is the average of RC1-3-7, RC2-3-7, and RC3-3-7. This format streamlines analysis by summarizing the performance of replicate samples under the same mix and curing condition.

www.naujcve.com. All Rights Reserved 2025.

Compressive Strength = Failure Load/ Area of cube (MPa or N/mm^2)

$$\text{Compressive Strength} = \frac{\text{Failure Load}}{\text{Area of Cube}} \quad (3.1)$$

Compressive Strength Trends

Results indicate a consistent decrease in compressive strength with higher rubber content. Rubber crumbs, due to their hydrophobic nature and lower bonding capacity, disrupt the geopolymer matrix, leading to weaker mechanical properties. For unrubberized samples, compressive strength values remained below conventional concrete standards due to the limited SiO^{4-} and Al^{3+} content in GGBFS.

i.Quantitative Relationships:

A regression analysis was performed to identify the relationship between rubber crumb content and compressive strength.

The simple linear regression model for the relationship between compressive strength (y) and the percentage of tyre dust (x) is,

$$y = 0.1796 - 0.0089x \quad (3.2)$$

Where:

y = Compressive strength (MPa)

x = Rubber content (%)

The correlation coefficient is −0.923, indicating a strong negative relationship between tyre dust content and compressive strength and the model adequacy (R2) value is 0.853 which signifies 85.3% of the variation in compressive strength is explained by the percentage of tyre dust. The model is statistically significant ($p<0.001$). The Residual Plot Model for compressive strength model is as shown in Fig. 3.6.

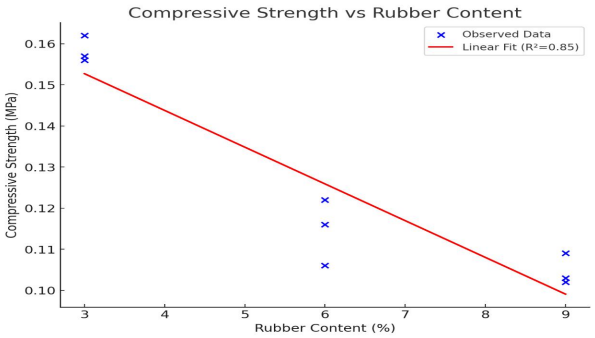

Fig.3.6 Residual Plot for Compressive Strength Model

ii.Significance Testing:

a.An ANOVA test indicated statistically significant differences ($p < 0.05$) between compressive strengths at 3%, 6%, and 9% rubber content. This reinforces the hypothesis that rubber crumbs significantly affect the structural integrity of GPC.

Where: p is p-value = statistically significant difference between group means

Benchmarking the findings from this research on rubberized geopolymer concrete against previous studies reveals similar trends. For instance, Ahmad et al., [19] reported linear patterns, such as the reduction in compressive strength with increasing rubber content, which correspond with the regression analysis results of this study. Similarly, it was documented that the effects of partially replacing conventional materials with crumb rubber and silica fume, paralleling the influence of tire crumbs and GGBFS in this work, highlighting the linear relationship between rubber content, workability, and strength.

To enhance the performance of rubberized GGBFS geopolymer concrete, it is recommended to supplement GGBFS with aluminosilicate-rich materials like fly ash or metakaolin, and to pre-treat rubber crumbs for better matrix bonding. Optimizing mix designs for specific applications and collaborating with industry stakeholders will support practical implementation and promote sustainable construction practices.

www.naujcve.com. All Rights Reserved 2025.

IV. CONCLUSIONS

This research aimed at evaluating the mechanical properties and behavior of rubberized GGBFS-based GPC and the followings can be concluded from the investigation:

1.Compressive strength decreased with increasing rubber content with an average reduction of 40-50% at 9% rubber content compared to unrubberized GPC and 3% replacement level showed the best balance between mechanical performance and sustainability.

2.Regression analysis between compressive strength and rubber content highlighted a strong negative correlation. While FTIR revealed weak bonding between rubber crumbs and the geopolymer matrix due to hydrophobic properties and limited aluminosilicate availability, the GGBFS used in the study contained low levels of reactive SiO_2 and Al_2O_3, limiting geopolymerization and contributing to reduced mechanical properties.

3.By comparison, Unrubberized GPC higher compressive strength 2.230MPa compared to 0.156 MPa (3% rubber), 0.106 MPa (6% rubber), and 0.102 MPa (9% rubber) at 28 days. Unrubberized GPC outperformed rubberized variants significantly, with the modulus of rupture declining from 4.17 MPa to 0.51 MPa as rubber content increased. In similar trend unrubberized samples achieved 2.5 MPa, while 9% rubber content reduced tensile strength to 1.2 MPa

4. Use of waste tire crumbs addresses environmental concerns by recycling rubber waste and reducing dependency on natural aggregates. At optimal replacement, is suitable for lightweight, non-structural applications due to its balance between cost savings and mechanical performance through reduced material costs.

REFERENCES

[1] John, T., and Smith, R. (2021). Integration of industrial by-products in concrete: Reducing carbon footprint while enhancing mechanical properties. Journal of Sustainable Construction Materials, Vol.34, No.2, Pp 123-135.

[2] Lateef, N. A., Kealy, C., Edward, D., and Paul, Z. (2020). A review of availability of source materials for geopolymer/sustainable concrete. Journal of Cleaner Production, Vol.263, 121477.

[3] Devi, K. S., Lakshmi, V. V., and Alakanandana, A. (2017). Impact of cement industry on environment: An overview. Asia Pacific Journal of Research, Vol.1, No.57, Pp 156-161.

[4] McLellan, B. C., Williams, R. P., Lay, J., Van Riessen, A., and Corder, G. D. (2011). Costs and carbon emissions for geopolymer pastes in comparison to ordinary Portland cement. Journal of Cleaner Production, Vol.19, No.9, Pp 1080-1090.

[5] Emad, B., Ezzatollah, S., and Muhammad, I. R. (2021). Challenges against CO2 abatement strategies in cement industry: A review. Journal of Environmental Sciences, Vol.104, Pp 84-101.

[6] Sharbatdar, M. K., Abbasi, M., and Fakharian, P. (2020). Improving the properties of self-compacted concrete with combined silica fume and metakaolin. Journal of Periodica Polytechnica Civil Engineering, Vol.64, No.2, Pp 535-544.

[7] Lloyd, N. A., and Rangan, B. V. (2019). Geopolymer concrete with fly ash. Proceeding of Second International Conference on Sustainable Construction Materials and Technologies, Ancona, June, 2019.

[8] Sherin, H. K., and Riyadh, A. (2022). Marine geopolymer concrete – A hybrid curable self-compacting sustainable concrete for marine applications. Journal of Applied Science, Vol.12, No.6, Pp 3116.

[9] Mehta, A., and Siddique, R. (2018). Sustainable geopolymer concrete using ground granulated blast furnace slag and rice husk ash: Strength and permeability properties. Journal of Cleaner Production, Vol.205, Pp 49-57.

[10] Nath, P., and Sarker, P. K. (2017). Fracture properties of GGBFS-blended fly ash geopolymer concrete cured in ambient temperatures. Materials and Structures, Vol.50, No.1, Pp 32.

[11] Hadi, M. N. S., Farhan, N., and Sheik, M. N. (2017). Design of geopolymer concrete with GGBFS at ambient curing condition using the Taguchi method. Construction and Building Materials, Vol.140, Pp 424-431.

[12] Glasby, T., Day, J., Genrich, R., and Aldred, J. EFC Geopolymer Concrete Aircraft Pavements at Brisbane West Wellcamp Airport. Proceedings of the 27th Biennial National Conference of the Concrete Institute of Australia in conjunction with the 69th RILEM Week, Melbourne, September, 2015.

[13] Mohabbi, M., and Dener, M. (2021). Investigation of elevated temperature on compressive strength and microstructure of alkali-activated slag-based cements. European Journal of Environmental and Civil Engineering, Vol.25, No.5, Pp 924–938.

www.naujcve.com. All Rights Reserved 2025.

[14] Reddy, D. V., Edouard, J. B., and Sobhan, K. (2013). Durability of fly ash–based geopolymer structural concrete in the marine environment. Journal of Materials in Civil Engineering, Vol.25, No.6, Pp 781–787.

[15] Ahmed, M., Khan, S., and Iqbal, R. (2023). Enhancing ductility and crack resistance in rubberized geopolymer composites. Construction and Building Materials, Vol.410, Pp 129876.

[16] Martauz, P., and Vaclavik, V. (2021). Advances in geopolymer materials. IOP Conference Series: Earth and Environment Science, Ho Chi Minh, November, 2021.

[17] Ediae, J. O., and Okovido, J. O. (2016). Geopolymer concrete mix designs. Retrieved from https://www.academia.edu/38843622/Jounal_2. Accessed 7 December 2022.

[18] Gayathri, K., and Raja, J. (2020). An experimental investigation on partial replacement of crumbs rubber for sand and silica fume for cement in concrete. International Research Journal of Engineering and Technology, Vol.7, Pp 645-654.

[19] Ahmad, J., Zhou, Z., Majdi, A., Alqurashi, M., and Deifalla, A. F. (2022). Overview of concrete performance made with waste rubber tires: A step toward sustainable concrete. Materials, Vol.15, No.16, Pp 5518.

www.naujcve.com. All Rights Reserved 2025.